arXiv:1211.6869v1 [physics.acc-ph] 29 Nov 2012

Correction of beam-beam effects in luminosity measurement at ILC

S. Lukić and I. Smiljanić

November 30, 2012

Abstract

Three methods for handling beam-beam effects in luminosity measurement at ILC are tested and evaluated in this work. The first method represents an optimization of the LEP-type asymmetric selection cuts that reduce the counting biases. The second method uses the experimentally resonstructed shape of the $\sqrt{s'}$ spectrum to determine the Beamstrahlung component of the bias. The last, recently proposed method, relies on the reconstruction of the collision-frame velocity to define the selection function in the collision frame both in experiment and in theory. Thus the luminosity expression is insensitive to the difference between the CM frame of the collision and the lab frame. Both the second and the third method are accurate to better than one permille of the total luminosity, but the collision-frame method has the distinct advantage of being independent of the knowledge of the beam parameters. The compatibility of diverse selection cuts for background reduction with the collision-frame method is addressed.

1 Introduction

Luminosity and luminosity spectrum are key data in analyses of most measurements at a Linear Collider, including mass and cross-section measurements, as well as the production-threshold scans. Precision measurement of luminosity is thus essential for the physics programme at a Linear Collider. The standard way to measure luminosity is to count Bhabha-scattering events recognized by coincident detection of showers in the two halves of the Luminometer in the very forward region in a given angular and energy range. The number of events N is then divided by the Bhabha cross section σ integrated in the corresponding region of the phase space.

$$L = \frac{N(\Xi(\Omega_1^{lab}, \Omega_2^{lab}, E_1^{lab}, E_2^{lab}))}{\sigma(\Xi^*(\Omega_1^{CM}, \Omega_2^{CM}, E_1^{CM}, E_2^{CM}))}, \qquad (1)$$

Here $\Xi(\Omega_1^{lab}, \Omega_2^{lab}, E_1^{lab}, E_2^{lab})$ are the selection criteria for counting the detected events, and $\Xi^*(\Omega_1^{CM}, \Omega_2^{CM}, E_1^{CM}, E_2^{CM})$ is the corresponding region of phase space where the cross section is integrated. The functions Ξ and Ξ^* are often expressed as the product of several functions ζ_i and ζ_i^* that are based on specific kinematical properties of the detected/generated pair.

Bhabha scattering is a well known QED process, for which cross-section calculations with relative uncertainty better than 10^{-3} are available [1]. However, one may note that Ξ i Ξ^* operate on kinematical arguments in different reference frames. The cross section is typically calculated by Monte Carlo integration using an event generator in the CM frame of the process. On the other hand, the experimentally detected Bhabha particles are affected by the beam-beam effects at bunch collision [2, 3]. Because of the random and asymmetric momentum loss when electrons emit Beamstrahlung, the CM frame of the Bhabha process is different for every colliding pair, and in general it does not coincide with the laboratory frame. As a consequence, the angles and energies of the outgoing particles seen in the laboratory frame are different than in the CM frame. Therefore, if the selection criteria are applied in the same form for the detected events as for the cross-section integration, different regions of the phase space will be covered, leading to a systematic bias in the luminosity measurement.

At LEP, this problem was usually addressed by designing ”asymmetric” selection cuts to minimize the beam-beam effects on the Bhabha counting rate [4, 5, 6]. Similar techniques were proposed for ILC as well, where the beam-beam effects are much more intense [7, 8]. In this context, Rimbault et al. also proposed to use the experimentally reconstructed form of the $\sqrt{s'}$ spectrum to determine the remaining counting bias [8]. Two methods based on these two concepts will be presented here, and their effectivenes will be tested.

Finally, a recently proposed way of handling the beam-beam effects will be tested for ILC [9]. The guiding idea of the new method is to define Ξ and Ξ^* such that the counting rate is independent of the reference frame. This can be achieved by expressing some of the factors ζ_i and ζ_i^* in terms of Lorentz-invariant kinematic parameters, and/or by designing ζ_i and ζ_i^* in such a way that the reconstructed experimental count and the cross-section integration limits are defined in the same reference frame. If these conditions are met, the luminosity measurement is insensitive to the difference of the CM frame and the lab frame, and requires no correction by beam-beam simulation, and no precise knowledge of beam parameters.

In Sec. 1.1, the physical processes affecting the luminosity measurement will be outlined, and the event simulation methods used in this work will be briefly described. In Sec. 2, the three methods of handling the beam-beam induced counting bias will be described and tested on simulated events. In Sec. 3, the compatibility of the collision-frame method with various additional selection cuts of interest for background removal is discussed. In the conclusions, the performance of these methods for the final precision of the luminosity measurement will be summarized, and the methods will be evaluated based on these results, but also based on the (in)dependence of the method on the parameters determined by simulation.

1.1 The physical processes affecting the luminosity measurement

Beamstrahlung

Due to the pinch effect during the bunch collision, particles from both bunches may emit Beamstrahlung photons and so lose energy and momentum before the interaction. Thus, in general, the center-of-mass (CM) energy of an electron-positron pair is smaller than the nominal energy of the collider $E_{CM} < E_0 \equiv 2E_{beam}$. The center-of-mass (CM) energy distribution at this stage is the actual luminosity spectrum $\mathcal{L}(E_{CM})$. The probability of the Bhabha scattering scales with $1/E^2_{CM}$, resulting in the CM energy distribution of the Bhabha events $\mathcal{B}(E_{CM}) \propto \mathcal{L}(E_{CM})/E^2_{CM}$.

Beside that, due to the loss of momentum prior to the collision, the CM reference frame has a non-zero velocity with respect to the lab frame, and the detected particle angles θ_1^{lab} and θ_2^{lab} are boosted relative to the angles in the CM frame, which on average increases the acollinearity. In this way, Beamstrahlung induces an *angular counting loss* of Bhabha events.

Initial State Radiation

The Bhabha process is accompanied by emission of the initial-state radiation (ISR) that is nearly collinear with the initial particle momenta, as well as the final-state radiation (FSR) that is approximately collinear with the outgoing particle momenta. Since the ISR is nearly collinear with the beam axis, it misses the luminometer, so that the CM energy reconstructed from the detected particles is $E'_{CM} < E_{CM}$, and the corresponding spectrum can be represented as a generalized convolution of $\mathcal{B}(E_{CM})$ and the function describing the fractional CM energy loss due to the ISR.

In the CM frame of the two-electron system[1] after emission of ISR and before emission of the FSR, i.e. the *collision frame*, the deflection angles in the collision are the same for both particles, according to the momentum-conservation principle. One can, therefore, define a unique *scattering angle* θ^{coll}.[2] However, the loss of momentum due to ISR induces an additional relativistic boost in the outgoing particle angles in the same way as the Beamstrahlung. The detected angles are affected by the cumulative deformation from these two angular effects.

Finally the outgoing particles are deflected under the influence of the EM field of the bunches, thus inducing a small additional angular counting loss termed Electromagnetic Deflection (EMD) effect. Synchrotron radiation may be emitted in this process as well.

---

[1] Unless stated otherwise, electron always refers to electron or positron

[2] In reality, ISR and FSR can not be cleanly separated even theoretically, due to the quantum interference between them. Thus in practice, the collision frame is defined as the CM frame of the final electrons together with all radiation within a given tollerance angle with respect to the final electron momenta. The assumption of clean separation between ISR and FSR introduces a small uncertainty in the final result.

1.2 Event simulation methods

To test the analysis procedure, Bhabha events in the bunch-collision were simulated with the modified Guinea-PIG software [3] using a method resembling that by C. Rimbault et al. in Ref. [8]: After generating the initial four-momenta of the colliding e^-e^+ pairs, the decision is made by Guinea-PIG whether the Bhabha scattering will be realized in the collision, based on the $1/s$ proportionality of the Bhabha cross section. If a Bhabha event is to be realized, the final four-momenta are picked from a file generated at 3 TeV by the BHLUMI generator [10]. The momenta are then scaled to the CM energy of the colliding pair, rotated to match the collision axis, and then boosted back to the lab frame. Finally the outgoing Bhabha electrons are tracked to simulate the electromagnetic deflection. Events were generated with the scattering angle in the collision frame between 37 and 75 mrad.

The standard parameter set from the ILC Technical Progress Report 2011 [11] was used as the basis for both 500 GeV and 1 TeV. Beside the standard parameter set, simulations were also performed with variations of individual beam-parameters, in order to determine the influence of the beam-parameter uncertainties on the performance of the presented methods. The simulated beam-parameter variations include:

- Symmetric bunch size variations by ±10 and $\pm20\%$ and one-sided variations by +20% in each of the three spatial directions
- Symmetric charge variations by ±10 and $\pm20\%$ and one-sided +20% variation
- Beam offset in x- and y-direction by up to one respective bunch RMS width.

Thus in total, 25 sets of beam parameters were simulated for each of the two energy options. In each simulation, one single beam parameter was varied with respect to the standard parameter set. Between 1.5 and 4 million Bhabha events were generated in each simulation.

The interaction with the detector was approximated in the following way:

- The four-momenta of all electrons and photons that are collinear within 5 mrad after tracking, were summed together. The 5 mrad criterion corresponds closely to the Molière radius of the high-energy showers in the LumiCal [12]. The Beamstrahlung photons were not included as they are emitted close to the beam axis. For synchrotron radiation, the characteristic emission angles are of the order $1/\gamma$, which is smaller than 10^{-3} mrad for electron energies in the TeV range, therefore photon and electron four-vectors can be added.
- The energy resolution of the LumiCal was included by adding random fluctuations to the final particle energies. The random fluctuations were sampled from the Gaussian distribution with energy-dependent standard deviation [13, 14].
- The finite angular resolution of the LumiCal was included by adding random fluctuations to the final particle polar angles. The nominal value of $\sigma_\theta = 2.2 \times 10^{-5}$ estimated for the ILC version of LumiCal [12] was used.

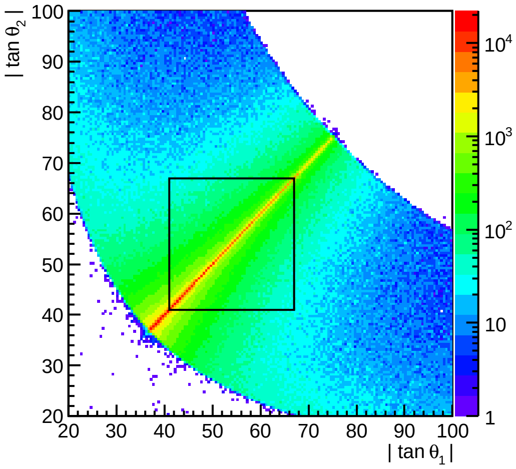

Figure 1: Scatter plot of the absolute values of polar angles of the outgoing Bhabha pairs in the Guinea-PIG simulation at 1 TeV. The thin black frame represents the angular limits of the FV. Events were generated with the scattering angle in the collision frame between 37 and 75 mrad.

Fig. 1 shows the scatter plot of the absolute values of polar angles of the outgoing Bhabha pairs in the Guinea-PIG simulation at 1 TeV. The angular limits of the nominal fiducial volume (FV) of the LumiCal are represented by the thin black frame in the figure. In the ILD design of the LumiCal, the FV is defined by the limiting angles $\theta_{\mathrm{min}} = 41$ mrad and $\theta_{\mathrm{max}} = 67$ mrad [15, 16].

The central diagonal representing collinear events is immediately recognizable in the figure due to the high number of collinear events. The density of events falls of rapidly with increasing acollinearity.

2 Correction methods

The first method presented here employs angular selection optimized in such a way that the components of the beam-beam induced counting bias partially cancel out, and the resulting bias is nearly insensitive to the variations in the beam parameters. This method will be termed the *compensation method*.

In the *luminosity-spectrum method*, the counting loss is determined from the ratio of the tail to peak integrals in the experimentally reconstructed $\sqrt{s'}$ spectrum.

In the *collision-frame method*, the velocity of the collision frame of the Bhabha scattering is experimentally determined, and the corresponding loss of acceptance relative to the collision frame is calculated and corrected event by event [9]. The resulting count N thus corresponds to the number of events with the scattering angle within the given limits in the collision frame, and the cross-section can be integrated within the same angular limits in the same reference frame.

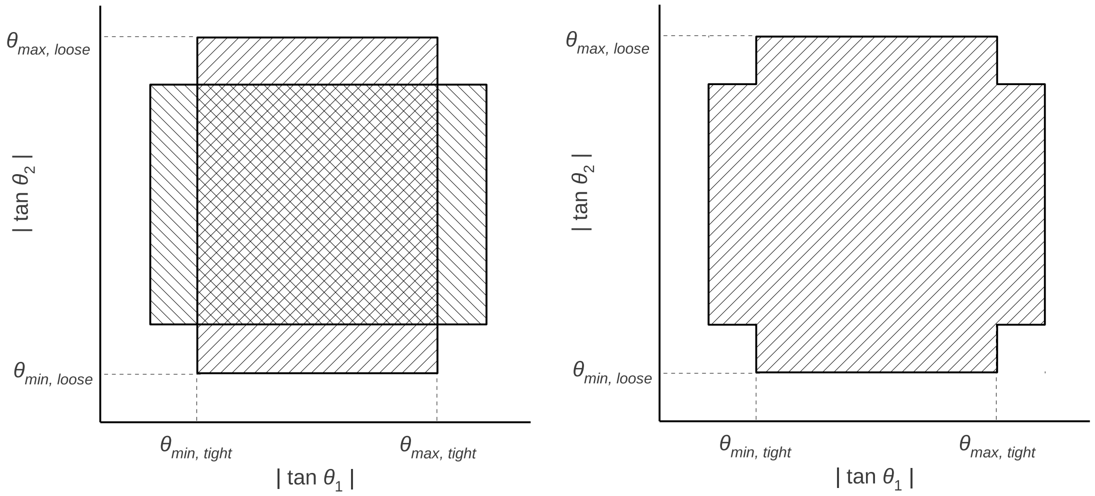

Figure 2: Schematic representation of the angular selection algorithms used at LEP. Left: the OPAL and the DELPHI collaborations, right: the L3 collaboration

Both the luminosity-spectrum method and the collision-frame method resolve the component of the counting bias due to Beamstrahlung. The method to separately determine the EMD component of the counting bias will be presented at the end.

2.1 The compensation method

At LEP, various "asymmetric" selection cuts were employed [4, 5, 6] to minimize the beam-beam effects on the Bhabha counting rate. Similar techniques were proposed for ILC, as well [7, 8]. In these techniques, two different angular cuts are applied at different side of the luminometer, one "tight" and one "loose". The tight cut typically corresponds to the FV of the luminometer, and the loose to the geometrical acceptance. Depending on which side of the tight cut is made, two asymmetric cuts, $\Xi_L(\theta_1, \theta_2)$ and $\Xi_R(\theta_1, \theta_2)$ are defined. In Refs. [4, 5, 7, 8], the arithmetic average of the counts obtained with Ξ_L and Ξ_R is used (Fig. 2, left). In that way, the effective relative weight assigned to the region corresponding to both particles being detected in the FV is twice as high as at the borders where only one particle is in the FV. In Ref. [6], the selection criterion is defined as logical OR between Ξ_L and Ξ_R, thus distributing the weight uniformly over a region shown in Fig. 2, right.

It has been shown that the application of the OPAL-type asymmetric selection algorithm effectively reduces the beam-beam effects at ILC [7, 8]. This can be intuitively understood if one considers that the loss of axial momentum in Beamstrahlung before the collision increases the acollinearity of the outgoing electrons, thus effectively displacing the coordinates of the pair along the direction perpendicular to the collinearity diagonal in the $|\tan\theta_1|$ vs. $|\tan\theta_2|$ space. The regions the most strongly affected by the counting loss due to this effect are in the vicinity of the lower-left and the upper-right corner in the diagram. Then the OPAL-type selection cuts allow for a partial recovery of the lost events in the border regions. We may also note that the

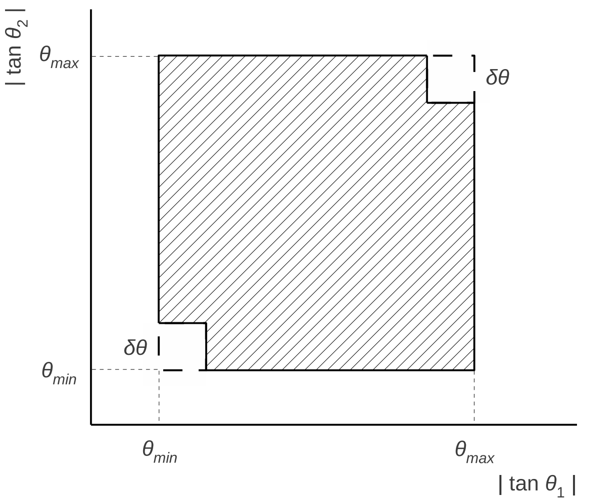

Figure 3: Schematic representation of the proposed angular selection algorithms. The solid line illustrates the modified selection criteria with the parameter $\delta\theta$

recovery of counts can be expected to be even more effective with the L3-type cuts (Fig. 2, right) due to the equal weighting of the border regions with respect to the FV. We also note that the upper-left and the lower-right corners do not play a significant role in the recovery of counts.

These considerations motivate the application of selection algorithms tailored specifically to optimize the counting loss. Such an algorithm can be constructed by requiring that both Bhabha particles be detected in the FV, except in the regions where both θ_1 and θ_2 fall either in the interval $(\theta_{min}, \theta_{min} + \delta\theta)$ or in the interval $(\theta_{max} - \delta\theta, \theta_{max})$, as shown in Fig 3. The topology of the selection is similar to the selection employed at L3, but no events are accepted outside of the FV in this scheme.

The parameter $\delta\theta$ can be optimized using simulations. Fig. 4 shows the total (Beamstrahlung and EMD) counting bias as a function of $\delta\theta$ for five different simulated bunch widths σ_x. Beside the possibility to reduce the counting loss to zero, it is worth noting that for certain values of $\delta\theta$, the variation of the count due to the variation of the beam parameters is minimal. When the entire set of beam imperfections described in Sec. 1.2 is taken into account, taking $\delta\theta = 5.6$ mrad in the 1 TeV case minimizes the maximum counting variation with respect to the standard beam parameters to 2.4 permille. Similarly, in the 500 GeV case, $\delta\theta = 4.6$ mrad results in the maximum counting variation of 2.8 permille.

Despite the somewhat reduced geometric counting efficiency, the four-year integral luminosity at ILC is sufficient to ensure statistic uncertainty better than 1×10^{-4} with this selection scheme.

2.2 Luminosity-spectrum method

It has already been shown that the form of the E_{CM} spectrum reconstructed from acollinearity of the outgoing pairs correlates with the counting loss due to Beamstrahlung [8]. To quantify the

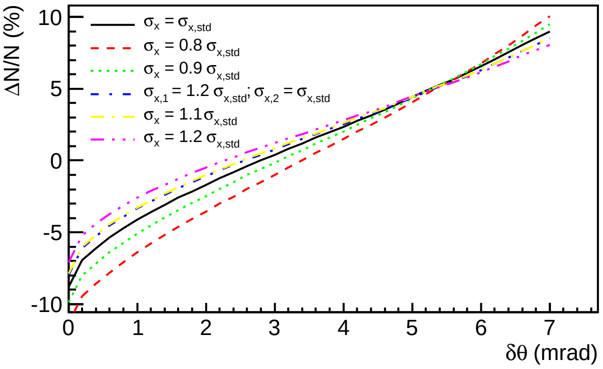

Figure 4: total counting bias (Beamstrahlung and EMD) as a function of $\delta\theta$ for five different σ_x bunch widths ranging from 80 to 120 % of the nominal σ_x.

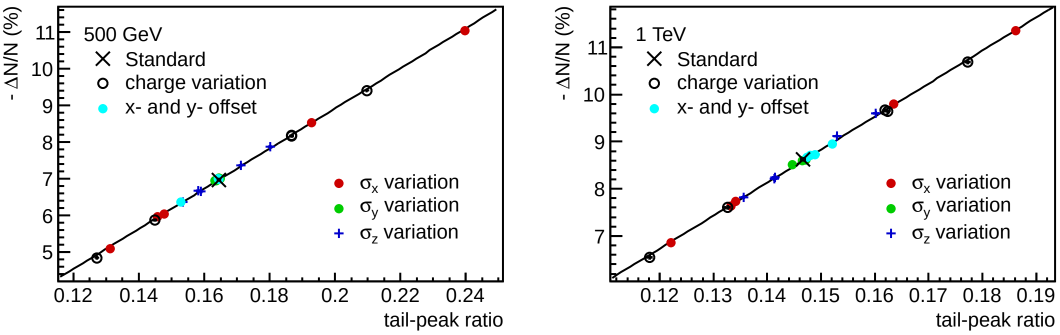

Figure 5: Correlation of the tail-to-peak ratio in the energy spectrum reconstructed from acollinearity to the Beamstrahlung counting loss for a diverse range of beam imperfections based on the standard parameter set from Ref. [11]. Left - ILC at 500 GeV, right - ILC at 1 TeV

correlation, the ratio of the integral in the tail to the peak is used in this work as the parameter of the form of the spectrum. The correlation to the counting loss is determined by simulation. Fig. 5 shows the results at 500 GeV and 1 TeV for the whole range of simulated beam imperfections described in Sec. 1.2. The angular selection included the whole FV on both sides. In the 500 GeV case, the tail integral was calculated in the range from 400 to 475 GeV, and the peak integral from 475 GeV upwards. In the 1 TeV case, the tail was integrated from 800 to 940 GeV, and the peak from 940 GeV upwards. The energy ranges of the tail and the peak are optimized to ensure a correlation that is as linear as possible, when all types of beam imperfections are included. This is important in order to be able to estimate the Beamstrahlung in the integral measurement from the mean value of the tail-to-peak ratio, regardless of the fluctuations of the bunch parameters.

In the 500 GeV case, the maximum residual difference of the simulated Beamstrahlung from the fitted values is 0.86 permille of the total luminosity, and in the 1 TeV case, 0.79 permille of the total luminosity. The deviations for all points correspond well to expected deviations from the statistical uncertainties of the simulated counting bias, and the errors of the fit parameters. This implies that with increased statistic, smaller residual deviations can be expected. The robustness of the correlation of the tail-to-peak ratio to the Beamstrahlung component of the counting loss, regardless of the specific type of beam imperfection, gives this parameter credibility for accurate correction of the Beamstrahlung effect.

2.3 Collision-frame method [9]

As already noted in Sec. 1.1, in the collision frame the deflection angles of both colliding particles are the same due to the momentum conservation principle. The movement of the collision frame with respect to the lab frame is responsible for the acollinearity leading to the angular counting loss. Since the kinematics of the detected showers correspond to the system after ISR, the velocity of the collision frame $\vec{\beta}_{coll}$, can be calculated to a good approximation from the measured polar angles. If β_{coll} is taken to be collinear with the z-axis, the expressions for the boost of the Bhabha scattering angles into the lab frame give,

$$\beta_{coll} = \frac{\sin(\theta_1^{lab} + \theta_2^{lab})}{\sin\theta_1^{lab} + \sin\theta_2^{lab}} \tag{2}$$

Due to the increase of acollinearity, the effective acceptance of Bhabha events in the luminometer decreases with increasing β_{coll}. The effective limiting scattering angles θ_{min}^{coll} and θ_{max}^{coll} in the collision frame for a given β_{coll} are obtained by boosting θ_{min} and θ_{max} into the collision frame. This allows calculating the event-by-event weighting factor to compensate for the loss of acceptance,

$$w(\beta_{coll}) = \frac{\int\limits_{\theta_{min}}^{\theta_{max}} \frac{\mathrm{d}\sigma}{\mathrm{d}\theta}\,\mathrm{d}\theta}{\int\limits_{\theta_{min}^{coll}}^{\theta_{max}^{coll}} \frac{\mathrm{d}\sigma}{\mathrm{d}\theta}\,\mathrm{d}\theta}. \tag{3}$$

To test this correction procedure, histograms of $E_{CM,rec}$ reconstructed from the full kinematical information of the detected particles, were generated in the following way:

Control histogram : All events with the scattering angle in the collision frame θ^{coll} such that $\theta_{min} < \theta^{coll} < \theta_{max}$ are accepted. Therefore this histogram is not affected by counting losses due to Beamstrahlung and ISR. This is, of course, only possible in the simulation.

Uncorrected histogram : Events hitting the FV of the LumiCal in the lab frame.

Corrected histogram : Events hitting the FV of the LumiCal in the lab frame, stored with the weight w calculated according to Eq. 3

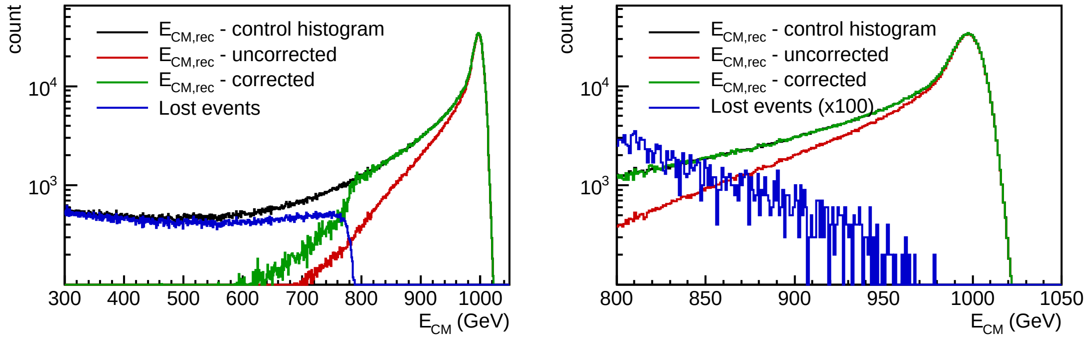

Figure 6: Correction of the counting loss due to Beamstrahlung and ISR at 1 TeV. Left: whole spectrum; right: zoom on energies above 800 GeV. Black: Simulated control spectrum without counting loss due to Beamstrahlung and ISR; red: Reconstructed E_{CM} spectrum affected by the counting loss; green: Reconstructed spectrum with correction for the counting loss due to Beamstrahlung and ISR; blue: events inaccessible to the correction

To calculate the correction weight w, the approximate expression for the angular differential cross section $d\sigma/d\theta \approx \theta^{-3}$ was used.

The results are shown in Fig. 6 for the 1 TeV case. The control spectrum is plotted in black, the spectrum affected by the counting loss in red, the corrected spectrum green. The blue line represents the events inaccessible to the correction due to the high value of $\beta_{coll.}$. The subsets of events characterized by $\beta_{coll.}$ above a certain treshold do not intersect the FV anymore [9]. These subsets can not be corrected by this method. However, for such events, the Beamstrahlung-ISR energy loss is also above a certain minimum, so that they are only present in significant number below about 780 GeV. The presence of a small number of high-$\beta_{coll.}$ events at energies above 780 GeV is visible in the zoomed figure (Fig. 6, right), where these events are scaled by a factor 100. In these events, $\vec{\beta}_{coll}$ has a relatively high radial component, due to the off-axis radiation before collision. For these events, the assumption that $\vec{\beta}_{coll}$ is collinear with the beam axis is not valid [9]. The relative bias due to such events to the peak integral above 80% of the nominal CM energy is $(-1.29 \pm 0.03) \times 10^{-3}$ in the 1 TeV case, and $(-1.36 \pm 0.03) \times 10^{-3}$ in the 500 GeV case.

The following is the list of sources of systematic uncertainty of the present correction method:

- The assumption that $\vec{\beta}_{coll}$ is collinear with the beam axis,
- The use of the approximate angular differential cross section for the Bhabha scattering in the calculation of w,
- Assumption that all ISR is lost, and all FSR is detected, in the calculation of β_{coll} and w.

The first of these three sources of uncertainty is responsible for the presence of the "lost events" in the peak. It induces a systematic bias of ca. 1.3 permille of the peak count, which can only be corrected by beam-beam simulations. The variation of this bias with the beam-parameter variation is, however, smaller than 0.1 permille, indicating that a this effect can be reliably corrected. After adding this correction, the final deviations are compatible with zero to within their respective statistical uncertainties. The average final deviation was calculated for both energy options, for the entire set of simulations with variations of beam parameters (Sec. 1.2), taking the inverse square statistical uncertainty of the deviation as the weight. The average final deviation at 1 TeV is $(+0.10 \pm 0.10) \times 10^{-3}$, and at 500 GeV, the average final deviation is $(-0.01 \pm 0.09) \times 10^{-3}$.

The result of the luminosity measurement with this method is the number of events $N_{coll.}$ with scattering angles between θ_{min} and θ_{max} in the collision frame. The same limits can be used for the cross-section integration in the same reference frame. The initial CM energy supplied to the generator for the cross-section calculation should be sampled from the realistic form of the intrinsic luminosity spectrum $\mathcal{L}(E_{CM})$ (See Sec. 1.1). The form of $\mathcal{L}(E_{CM})$ can be determined either by simulation or by deconvolution of the ISR energy-loss from the measured spectrum.

2.4 Angular losses due to the EMD

The EMD shifts the polar angles of the outgoing particles consistently towards smaller angles. Since the Bhabha cross section is monotonously decreasing with the polar angle, the net effect of the EMD is a decrease in the Bhabha count. This effect is equivalent to a parallel shift in the angular limits θ_{min} and θ_{max} of the FV in the opposite direction by an *effective mean deflection* angle $\Delta\theta$.

$$\frac{\Delta L}{L} = \frac{1}{N}\frac{dN}{d\theta}\Delta\theta \tag{4}$$

The value of $\Delta\theta$ can be obtained by dividing the relative EMD counting loss obtained in the beam-beam simulation by the simulated or measured quantity $x_{EMD} = \frac{1}{N}\frac{dN}{d\theta}$, where N is the Bhabha count in the FV, and $d\theta$ denotes a parallel infinitesimal shift of both θ_{min} and θ_{max}.

Fig. 7 shows the fit of the $(dN/d\theta)_{sim}$ for the standard set of beam parameters at 1 TeV. $\Delta N = N_{shift} - N_{FV}$ is the difference in counts in the shifted angular cut $(\theta_{min} + \theta_{shift}, \theta_{max} + \theta_{shift})$, and the FV $(\theta_{min}, \theta_{max})$. The statistical errors of ΔN were estimated as $\delta(\Delta N) = \sqrt{n_{shift} + n_{FV}}$, where $N_{shift} = N' + n_{shift}$, $N_{FV} = N' + n_{FV}$ and N' is the number of events inside the intersection of the FV with the shifted angular cut. The slope at zero is $dN/d\theta = (7.519 \pm 0.015) \times 10^4\ \mathrm{mrad}^{-1}$. The number of counts in the FV in the simulation was 1.37×10^6, and the counting bias was $\Delta L_{EMD}/L = (-1.068 \pm 0.028)10^{-3}$. The resulting effective mean deflection is $\Delta\theta_{\mathrm{1TeV}} = (0.0194 \pm 0.0006)\ \mathrm{mrad}$.

In the 500 GeV case, the same procedure gives $\Delta\theta_{\mathrm{500GeV}} = (0.0426 \pm 0.0009)\ \mathrm{mrad}$.

If the simulated value of $\Delta\theta$ is returned to Eq. 4, it can be used in the experiment to correct for the EMD counting loss. The precision of this correction depends on the precision with which the beam parameters are known. Fig 8 shows the scatter plot of the values of the EMD counting loss obtained using a fixed simulated value of $\Delta\theta$ versus the "real" EMD loss in the

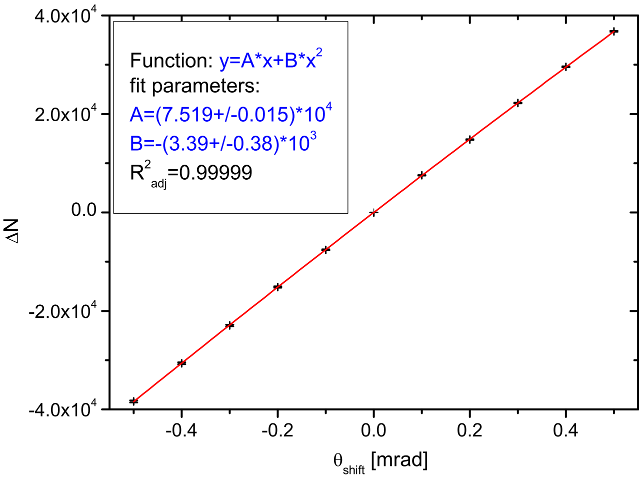

Figure 7: Fit of the $(dN/d\theta)_{sim}$ for the standard set of beam parameters at 1 TeV.

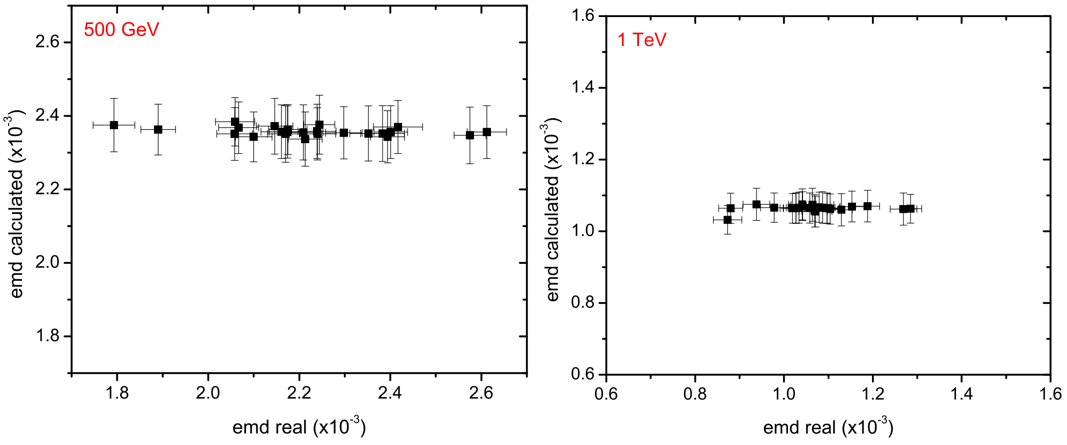

Figure 8: Scatter plot of the calculated EMD counting loss from $(dN/d\theta)_{sim}$ with a unique $\Delta\theta$ value derived for the nominal beam parameters, against the ”real” EMD obtained directly from the difference in counts for a diverse range of beam imperfections, including the bunch geometry, as well as the bunch charge variations. Left: the 500 GeV case, right: the 1 TeV case

simulation for each set of beam parameters, with individual parameter variations up to 20% as described in Sec. 1.2. The error of the counting-loss estimate due to the beam imperfections is always smaller than $\pm 5 \times 10^{-4}$ of the total luminosity in the 500 GeV case, and $\pm 2 \times 10^{-4}$ in the 1 TeV case. This represents a reduction of the uncertainty by a factor 5. If the beam parameters are known with better precision (see Ref. [17]), the uncertainty of the EMD effect is correspondingly smaller.

3 The collision-frame method and additional selection criteria

Because of the presence of background that can be falsely identified as Bhabha events in the luminosity measurement at a linear collider, there is a strong interest to apply additional cuts to limit the measurement to the region of phase space that is as free from background as possible. Several types of cuts are already well known from previous experiments. Beside the mentioned asymmetric polar-angle cuts, cuts on acoplanarity, acollinearity, minimum and average energy have been shown to effectively remove background [4]. Recently, the energy balance cut was also proposed [18].

In Sec. 2, it has been shown that the collision-frame method has distinct advantages both in the numerical precision, and in its essential independence of the simulation or the knowledge of the beam parameters. However, when additional selection cuts are considered, the independence of the beam parameters can be preserved only if the selection cuts are either based on the Lorentz-invariant quantities, or on quantities that are defined in the same reference frame in the experiment as well as in the cross-section integration. These conditions are satisfied in practice to a good approximation in two cases presented in the following.

3.1 Acoplanarity

The acoplanarity criterion is defined as $|\pi - |\phi_1 - \phi_2|| < \Delta\phi_{max}$. Although this criterion is based on the azimuthal angles of the detected particles, which are in general not Lorentz invariant, this criterion is to an excellent approximation invariant to the boost between the CM frame of the Bhabha event and the laboratory frame. The Beamstrahlung is so strongly forward-peaked that the corresponding boost nearly coincides with the beam axis. Beside this, the acoplanarity criterion suppresses events that have radiated significant off-axis ISR before collision. Therefore, it can be expected that the acoplanarity criterion reduces the fraction of lost events (Sec. 2.3).

In order to quantify these arguments, the collision-frame method was tested for the standard ILC parameter set with application of the acoplanarity criterion with several different values of $\Delta\phi_{max}$. The results are shown in Tab. 1. As can be seen from the table, the final numerical precision as well as the statistics are not affected by the application of the acoplanarity criterion. However, the fracton of lost events is reduced several times when the acoplanarity limit is set to 5 or 10 degrees.

Table 1: Relative final counting uncertainty, relative fraction of lost events, and the total statistic in the collision-frame method with application of the acoplanarity criterion for different values of $\Delta\phi_{max}$.

$\Delta\phi_{max}(^\circ)$	$\left(\frac{\Delta N}{N}\right)_{final}$ 10^{-3}	$\left(\frac{\Delta N}{N}\right)_{lost}$ 10^{-3}	N 10^{6}
π (any acoplanarity accepted)	+0.50±0.48	1.34±0.03	1.358
57.3	+0.64±0.49	1.18±0.03	1.358
10	+0.17±0.48	0.59±0.02	1.354
5	+0.65±0.48	0.36±0.02	1.346

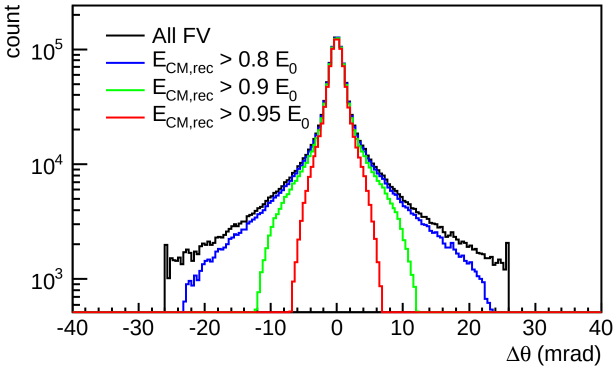

Figure 9: Distribution of $\Delta\theta = \theta_2 - \theta_1 - \pi$ for several different cuts on E_{CM}. Black line: no E_{CM} cut – all events in FV accepted; blue: events with $E_{CM} > 0.8E_0$; green: events with $E_{CM} > 0.9E_0$; red: $E_{CM} > 0.95E_0$. Event weighting from the collision-frame method was applied.

It can be concluded that the acoplanarity criterion can be optimized for the needs of background reduction. The side effect of it is that it also reduces the fraction of lost events, thus enhancing the overall reliability of the measurement method.

3.2 Reduction of the acollinearity and the average energy ranges by the cut on CM energy

The average energy and the acollinearity criteria are not Lorentz invariant, and are based on quantities that are severely affected by the axial boost. However, these criteria can be effectively replaced by the cut on the reconstructed CM energy, which is strongly correlated both with the average energy of the two detected particles, and anticorrelated with the acollinearity. As already shown in Sec. 2.3, events with high reconstructed CM energy and high acollinearity are rare, and correspond to events with high off-axis radiation before collision.

As an illustration of the correspondence of the CM energy cut with the acollinearity cut, Fig.

9 shows the distribution of the parameter $\Delta\theta = \theta_2 - \theta_1 - \pi$ for several different cuts on E_{CM}. Event weighting from the collision-frame method was applied. Without the E_{CM} cut, $\Delta\theta$ is limited only by the requirement that the event falls within the FV. With the E_{CM} cut, the range of $\Delta\theta$ is progressively smaller when the E_{CM} cut is made nearer the peak, although the edges of the range are not sharp, as they would have been if the cut was made on $\Delta\theta$. In the tests in Sec. 2.3 and 3.1, the E_{CM} cut was always made at 80 % of the nominal energy. The exact position of the cut can be optimized if required for the background suppression.

4 Conclusions

Three methods for dealing with the beam-beam effects in the luminosity measurement were presented and tested using Monte Carlo event simulations. In the compensation method, the angular selection cuts are defined in such a way that the components of the counting bias partly compensate, and the resulting bias is almost insensitive to the beam-parameter variations, and can be directly corrected. In the remaining two methods, the EMD component of the bias is determined separately. The counting bias without correction, as well as the estimated precision of the correction for the three presented methods is listed in Tab. 2.

Table 2: Relative counting uncertainties after correction of the beam-beam effects using different methods.

Method	500 GeV (10^{-3})	1 TeV (10^{-3})
Uncorrected bias	-128	-140
Collision-frame method with corrections for the lost events and EMD	0.3	0.5
Luminosity spectrum and EMD correction	0.9	0.9
Compensation	2.8	2.3

The presented methods allow reaching precision of the order of permille or better in the luminosity measurement at ILC for both 500 GeV and 1 TeV, in the experimental situation where the key bunch parameters are known with a precision of 20%. The uncertainty of the collision-frame method is the best, even though it is dominated by the uncertainty of the EMD correction. The proposed EMD correction has the weakness that the effective deflection $\Delta\theta$ is not directly measured, but has to be estimated from simulation. For this, knowledge of beam parameters is necessary, and the method is sensitive to their uncertainties. However, as the EMD component of the bias is small at the outset, the final uncertainty seems to be acceptable.

To maintain the robustness of the collision-frame method, the choice of additional selection cuts for background removal is limited to cuts expressed in quantities that are invariant under the Lorentz boost from the CM frame to the lab frame. Two examples of such cuts were tested. In particular, the acoplanarity cut improves the condition related to the high-energy "lost events" due to the off-axis component of the ISR.

The collision-frame method results in the number of events N in the angular range $(\theta_{min}, \theta_{max})$ defined in the collision frame. The same limits can be used for the cross-section integration in the same reference frame. Thus the luminosity expression (Eq. 1) can be written in a way that is essentially insensitive to the variation of the CM frame induced by the beam-beam effects. In this way, beam-beam simulation remains necessary only for the correction of the EMD effect, and of the high-energy "lost events". Both these effects are of the order of 1 or 2 permille, while the main component of the beam-beam related counting bias is resolved in a theoretically solid, and experimentally robust way, independent of the simulation and of the knowledge of the beam parameters.

References

[1] S. Jadach *Theoretical error of luminosity cross section at LEP*, 2003 (arXiv:hep-ph/0306083).

[2] K. Yokoya and P. Chen, *Beam-beam phenomena in linear colliders,* in Frontiers of Particle Beams: Intensity Limitations, Vol. 400 of *Lecture Notes in Physics* Springer Verlag, 1991, pp. 415–445 (US-CERN School on Particle Accelerators).

[3] D. Schulte, *Study of Electromagnetic and Hadronic Background in the Interaction Region of the TESLA Collider,* PhD thesis, Hamburg University, 1996.

[4] OPAL Collaboration, *Precision luminosity for Z0 line shape measurements with a silicon tungsten calorimeter,* Eur.Phys.J. **C14** (2000), 373–425.

[5] ALEPH Collaboration, *Measurement of the Z resonance parameters at LEP,* Eur.Phys.J. **C14** (2000), 1–50.

[6] L3 Collaboration, *Measurements of cross-sections and forward backward asymmetries at the Z resonance and determination of electroweak parameters,* Eur.Phys.J. **C16** (2000), 1–40.

[7] A. Stahl *Luminosity measurement via Bhabha scattering: Precision requirements for the luminosity calorimeter* Technical Report LC-DET-2005-004, SLAC, 2005.

[8] C. Rimbault, P. Bambade, K. Mönig, and D. Schulte, *Impact of beam-beam effects on precision luminosity measurements at the ILC,* Journal of Instrumentation **2** (2007), P09001.

[9] S. Lukić *Correction of systematic uncertainties due to beam-beam effects in luminosity measurement in LumiCal at CLIC* Technical Report LCD-Note-2012-008, Linear Collider Detector project, CERN, 2012.

[10] S. Jadach, W. Placzek, E. Richter-Was, B. Ward, and Z. Was, *Upgrade of the Monte Carlo program BHLUMI for Bhabha scattering att low angles to version 4.04,* Computer Physics Communications **102** (1997), 229.

[11] ILC Collaboration *International Linear Collider - A technical progress report* Technical Report ILC-REPORT-2011-30, International Linear Collider, 2011 (ISBN: 978-3-935702-56-0).

[12] I. Sadeh *Luminosity measurement at the International Linear Collider* Master's thesis, Tel Aviv University, 2008.

[13] R. Schwartz, *LumiCal performance in the CLIC environment - progress report*, in Proceedings of the 18th FCAL Workshop in Predeal, Romania, 2011, p. 84.

[14] (L. Linssen, A. Miyamoto, M. Stanitzki, and H. Weerts, eds.), *Physics and Detectors at CLIC*, CERN European organization for nuclear research, 2012 (CLIC Conceptual Design Report, CERN-2012-003).

[15] ILD Concept Group *The International Large Detector - Letter of Intent* Technical Report DESY 2009/87 - Fermilab PUB-09-682-E - KEK Report 2009-6, DESY / KEK / Fermilab, 2010 (ISBN: 978-3-935702-42-3, http://ilcild.org/documents/ild-letter-of-intent/).

[16] H. Abramowicz et al., *Forward instrumentation for ILC detectors*, Journal of Instrumentation **5** (2010), P12002.

[17] C. Grah and A. Sapronov, *Beam parameter determination using beamstrahlung photons and incoherent pairs*, Journal of Instrumentation **3** (2008), P10004.

[18] M. Pandurović, *Fon u merenju luminoznosti i razvoj metode za identifikaciju b-kvarka u eksperimentima ILC i H1*, PhD thesis, Univerzitet u Beogradu, 2011.